Intra-excitonic relaxation dynamics in ZnO

Alexej Chernikov,[1] Martin Koch,[1] Bernhard Laumer,[2] Thomas A. Wassner,[3] Martin Eickhoff,[2,a)] Stephan W. Koch,[1] and Sangam Chatterjee[1]
[1]*Fachbereich Physik, Philipps-Universität Marburg, D-35032 Marburg, Germany*
[2]*I. Physikalisches Institut, Justus-Liebig-Universität Giessen, Heinrich-Buff-Ring 16, 35392 Giessen, Germany*
[3]*Walter Schottky Institut, Technische Universität München, Am Coulombwall 3, 85748 Garching, Germany*

(Received 20 July 2011; accepted 14 November 2011; published online 9 December 2011)

The temperature and carrier-density dependent excitonic relaxation in bulk ZnO is studied by means of time-resolved photoluminescence. A rate-equation model is used to analyze the population dynamics and the transitions between different exciton states. Intra-excitonic (n = 1) to (n = 2) relaxation is clearly identified at low excitation densities and lattice temperatures with a characteristic time constant of 6 ± 0.5 ps. © *2011 American Institute of Physics*.
[doi:10.1063/1.3668102]

Over the last decades, ZnO has attracted much interest in the scientific community mainly due to its potential application for optoelectronic devices in the ultraviolet (UV) spectral regime. In addition, properties associated with the large exciton binding energy of 60 meV and the strong electron-phonon coupling are of fundamental interest.[1] Recently, high quality ZnO samples have become available due to improved growth methods.[2–6] These advances allow for accurate studies of the electro-optical properties of the material and are important steps towards the realization of ZnO-based technology. Significant research effort has been directed towards the growth and applications of quantum well structures,[7,8] ternary ZnO-based compounds,[9–12] electron-phonon interaction,[13] and exciton-polaritons.[14] Even steady-state investigations of the excited excitonic states have become possible.[15,16]

In this letter, we study the dynamics of the intra-excitonic processes by means of ultrafast emission spectroscopy with sub-picosecond time resolution. We apply a rate-equation model to analyze the various relaxation channels and to investigate the influence of temperature and excitation density.

All time-resolved photoluminescence (PL) measurements are performed using a streak-camera setup[12] yielding spectral and time resolutions of 0.15 nm and 500 fs, respectively; a pulsed 100 fs-Ti:sapphire laser is used as an excitation source. The investigated sample is a 300 nm thick c-plane ZnO layer grown by plasma-assisted molecular beam epitaxy.[11] The emission signal is collected normally to the sample surface in reflection geometry. Structural analysis by high resolution x-ray diffraction was carried out and the lattice parameters were extracted from reciprocal space maps recorded at the asymmetric (20.5) reflex. The c-lattice parameter was determined to (5.2046 ± 0.001) and the a-lattice parameter to (3.2515 ± 0.001). Comparison to data reported in literature reveals that the present ZnO layer can be considered as unstrained.[17]

Figure 1 shows the PL spectrum at a lattice temperature of T = 10 K, integrated over the first 20 ps after the excitation. The pump fluence per pulse is set to 1.5×10^{11} photons/cm^2 and the photon energy to 4.2 eV. As usual, donor bound excitons (DX) at 3.359 eV dominate the overall emission.[18] Additionally, luminescence from the (n = 1) states of the free A-excitons is observed at 3.376 eV ($FX_A^{(n=1)}$). The shoulder on the high energy side of the $FX_A^{(n=1)}$ transition is attributed to the luminescence of the free B-excitons. Also, an additional, distinct emission peak is found at 3.423 eV. In a simplified picture, the excitonic level scheme resembles the energy structure of a hydrogen atom.[1] In this case, the energy of an excited states is proportional to $\frac{E_b}{n^2}$, where E_b is the binding energy and n is the quantum number of the corresponding state. Thus, the energy of the first excited state with (n = 2) is 1/4 E_b and the separation between the (n = 1) and (n = 2) states equals 3/4 E_b. Here, the energy spacing of 47 meV of the peak at 3.423 eV from the $FX_A^{(n=1)}$ at 3.376 eV matches exactly 3/4 of the exciton binding energy in ZnO. Therefore, the transition at 3.423 eV, also reported in the literature,[14–16,19,20] is attributed to the (n = 2) state of the A-exciton. A magnification of the (n = 2) spectrum is shown enlarged on a linear scale in the inset of Fig. 1; a Lorenzian fit (grey-shaded area) yields its full-width-at-half-maximum (FWHM) of 10 meV. Hence, the lower

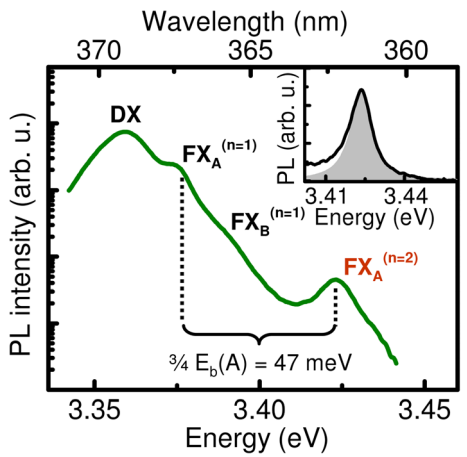

FIG. 1. (Color online) PL spectrum of the ZnO sample for the first 20 ps after the excitation. The lattice temperature is set to 10 K and the excitation fluence to 1.5×10^{11} photons/cm^2 per pulse. The inset shows a magnification of the $FX_A^{(n=2)}$ transition with the corresponding Lorenzian fit curve (grey-shaded area).

a)Author to whom correspondence should be addressed. Electronic mail: eickhoff@physik.uni-giessen.de.

limit for the decay dynamics of the (n = 2) resonance given by the uncertainty relation is $\tau_{decay}^{(n=2)} = 500$ fs, which is comparable to the time resolution of the experimental setup. The observation of the excited excitonic states in the emission spectrum confirms the high material quality of the sample.

The time-resolved data for the $FX_A^{(n=2)}$, $FX_A^{(n=1)}$, and DX transitions are shown in Fig. 2(a). The transients are spectrally integrated over a 10 meV range around the respective PL maxima and are normalized for better comparison. The (n = 2) emission develops first and, after several picoseconds, is followed by the (n = 1) transition. The decay of the (n = 2) PL is on the time-scale of several ps; the lifetime of the (n = 1) excitons is in the range of 20 ps. In comparison with the free excitons, the DX luminescence rises and decays more slowly.[21] To analyze the experimental data, we apply a rate equation model describing the relaxation and recombination dynamics

$$\dot{N}_2(t) = -\frac{N_2}{\tau_2} - \frac{N_2}{\tau_{21}} - \frac{N_2}{\tau_{2DX}} + \frac{N_1}{\tau_{12}} + \frac{N_{DX}}{\tau_{DX2}} + \frac{N_p}{\tau_p},$$
$$\dot{N}_1(t) = -\frac{N_1}{\tau_1} - \frac{N_1}{\tau_{12}} - \frac{N_1}{\tau_{1DX}} + \frac{N_2}{\tau_{21}} + \frac{N_{DX}}{\tau_{DX1}} + \frac{N_p}{\tau_p},$$
$$\dot{N}_{DX}(t) = -\frac{N_{DX}}{\tau_{DX}} + \frac{N_2}{\tau_{2DX}} + \frac{N_1}{\tau_{1DX}}.$$

Here, the time-dependent $FX_A^{(n=2)}$, $FX_A^{(n=1)}$, and DX populations are represented by N_2, N_1 and N_{DX}, respectively. The excitation pulse generates an initial carrier occupation N_p in the electron-hole continuum. Subsequently, exciton-polaritons are formed on a fast sub-ps time scale τ_p, as expected for II-VI wide-bandgap semiconductors due to the large exciton binding energy and strong carrier-phonon coupling.[1,22] Initially, the ground ((n = 1)) and the excited (e.g., (n = 2)) excitonic states are populated. The effective radiative recombination is usually slow in bulk materials due to the well-known polariton propagation effects.[1] Therefore, the decay of the excitonic PL is mainly governed by the relaxation to the shallow (e.g., DX) and deep impurities. The characteristic times for the DX capture are τ_{2DX} and τ_{1DX}. The remaining radiative and non-radiative recombination channels of the (n = 1), the (n = 2), and the DX states are summarized in the recombination times τ_2, τ_1, and τ_{DX}, respectively. In addition, the relaxation of the (n = 2) excitons to the (n = 1) states with a time-constant τ_{21} leads to a fast decay of the (n = 2) luminescence on a ps time scale. A finite temperature T also provides scattering upwards in energy, represented by $\tau_{12} = \tau_{21} \times e^{E_{21}/k_BT}$, $\tau_{DX2} = \tau_{2DX} \times e^{E_{2DX}/k_BT}$, and $\tau_{DX1} = \tau_{1DX} \times e^{E_{1DX}/k_BT}$. The rate-equations are solved numerically for the initial conditions N_p (0) = 1 and N_2 (0) = N_1 (0) = N_{DX} (0) = 0. E_{1DX}, E_{2DX}, and E_{12} are the energy separations between (n = 1), (n = 2), and DX states. The obtained transients are convoluted with a Gaussian, mimicking the temporal response of the experimental setup.

Fig. 2(b) shows the results of the rate-equation model and a simplified relaxation scheme on top of the graph. We obtain an excellent fit of the experimental data which allows us to extract the relevant relaxation times. According to this analysis, the carriers populate DX on a 25 ps scale and the effective recombination times τ_2, τ_1, and τ_{DX} are in the expected range of several 100 ps.[23–25] As the most interesting feature, we now focus on the relaxation dynamics between the excitonic (n = 2) and (n = 1) states both as a function of photon flux at T = 10 K and as a function of temperature at low excitation density of $n_0 = 1.5 \times 10^{11}$ photons/cm^2 per pulse. The corresponding PL spectra for the first 20 ps after the excitation are plotted in Figs. 3(a) and 3(b), respectively. The spectra are normalized and shifted for clarity. The (n = 2) peak broadens and the relative intensity of the (n = 2) and (n = 1) PL decreases at higher excitation densities and for increasing temperature. These observations are confirmed by the temperature dependence of the (n = 2) emission found in the literature.[16]

The extracted (n = 2) to (n = 1) relaxation times are shown in Figs. 4(a) and 4(b) as a function of excitation density and temperature, respectively. At low temperatures and densities, the simulation yields a relaxation time τ_{21} of 6 ± 0.5 ps. This remains nearly constant for lattice temperatures up to 50 K and low excitation densities. As either the excitation density or the temperature are increased, the intra-excitonic relaxation time is reduced. These findings rule out the observed decay of the (n = 2) PL is simply due to the cooling of the carrier system. Here, one would measure only

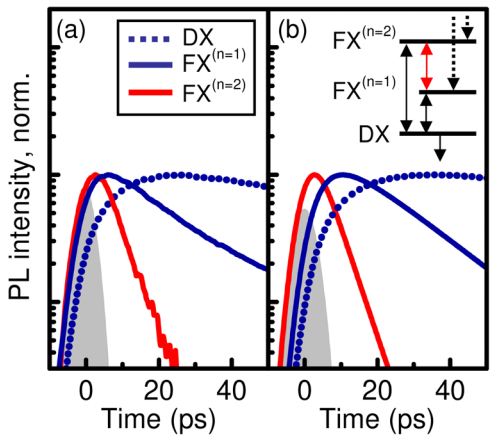

FIG. 2. (Color online) (a) Normalized transients of the $FX_A^{(n=2)}$, $FX_A^{(n=1)}$, and DX transitions. (b) Results of the rate-equation model. A simplified scheme of the model is shown on top of the graph. The detected excitation pulse corresponding to the temporal resolution of the setup is shown in grey.

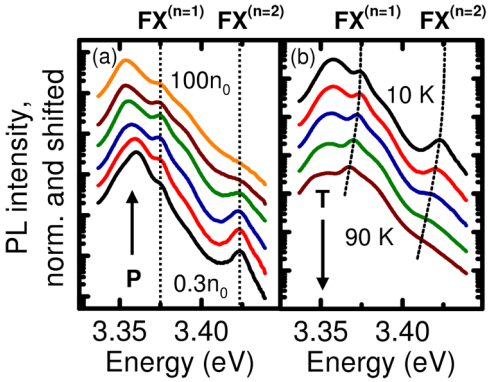

FIG. 3. (Color online) PL spectra as function of excitation density at T = 10 K with $n_0 = 1.5 \times 10^{11}$ photons/cm^2 per pulse (a) and as function of temperature for the constant photon flux n_0 (b). The excitation density and the temperature intervals are factors of 3 and 20 K, respectively. The spectra are normalized and shifted for clarity.

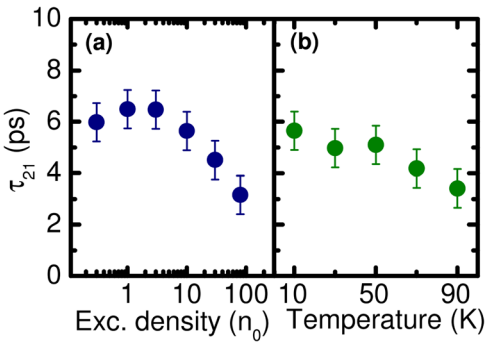

FIG. 4. (Color online) Relaxation time of the (n = 2) to (n = 1) excitonic transition as function of excitation density (a) and temperature (b).

the cooling rate instead of the pure relaxation time between the excited and ground states. However, in this case, the time constant τ_{21} should increase with both lattice temperature and excitation density due to elevated carrier temperatures and reduced cooling rates.[26–28] Instead, intrinsic scattering processes between the (n = 1) and the (n = 2) states are strongly suggested. In addition, the power and temperature dependence of the relaxation times indicate both Coulomb- and electron-phonon-scattering to influence the intra-excitonic relaxation.

Altogether, the relaxation of the (n = 2) excitons to the (n = 1) states is significantly faster than the majority of possible recombination and relaxation processes in the investigated temperature and density regime. These processes include capture to the shallow and deep impurities or propagation to the sample surface and subsequent radiative recombination. A possible additional recombination channel on the time scale of a few ps is the pure radiative recombination of (n = 2) excitons with sufficiently small momenta without any polariton propagation effects. The corresponding time constant is calculated by the evaluation of the radiative coupling[29] using the wavefunction of the (n = 2) excitonic state in position space.[30] With the material parameters of ZnO (Ref. 31), we obtain a recombination time of 5.2 ps. Therefore, this process has the potential to be a competing channel for the decay of the (n = 2) population in comparison to the intra-excitonic (n = 2) to (n = 1) relaxation. An influence of the pure radiative recombination on the carrier dynamics is thus expected in structures of reduced dimensionality under weak resonant excitation.[1]

In summary, we have studied the dynamics of the intra-excitonic processes in ZnO by time-resolved PL as function of excitation density and lattice temperature. The experimental data is analyzed using a rate-equation model. We obtain the intra-excitonic relaxation time between the (n = 2) and (n = 1) A-exciton states of 6 ± 0.5 ps for low excitation conditions and low temperatures. The (n = 2) to (n = 1) scattering dynamics become faster at higher pump densities and T ≥ 70 K. The experimental findings indicate that intrinsic scattering processes are responsible for the intra-excitonic relaxation between radiatively forbidden states. Additional experiments applying optical absorption-based techniques such as pump-probe[32] or THz spectroscopy[33] should provide further insight.

We thank C. N. Böttge, University of Marburg, for evaluating the radiative recombination times of the (n = 2) and (n = 1) exciton states. B.L. acknowledges financial support from the Universität Bayern e.V. A.C. and S.C also want to thank W. W. Rühle for helpful discussions.

[1] C. F. Klingshirn, *Semiconductor Optics*, 2nd ed. (Springer, Berlin, 2007).
[2] C. W. Teng, J. F. Muth, U. Özgür, M. J. Bergmann, H. O. Everitt, A. K. Sharma, and J. Narayan, Appl. Phys. Lett. **76**, 979 (2000).
[3] A. K. Sharma, J. Narayan, J. F. Muth, C. W. Teng, C. Jin, A. Kvit, R. M. Kolbas, and O. W. Holland, Appl. Phys. Lett. **75**, 3327 (1999).
[4] I. Park, G. C. Yi, and H. M. Jang, Appl. Phys. Lett. **79**, 2022 (2001).
[5] H. v. Wenckstern, H. Schmidt, C. Hanisch, M. Brandt, C. Czekall, G. Benndorf, G. Biehne, A. Rahm, H. Hochmuth, M. Lorenz, and M. Grundmann, Phys. Status Solidi (RRL) **1**, 129 (2007).
[6] S. Sadofev, P. Schäfer, Y. H. Fan, S. Blumstengel, F. Henneberger, D. Schulz, and D. Klimm, Appl. Phys. Lett. **91**, 201923 (2007).
[7] S. H. Park and D. Ahn, Appl. Phys. Lett. **87**, 253509 (2005).
[8] T. V. Shubina, A. A. Toropov, O. G. Lublinskaya, P. S. Kopev, S. V. Ivanov, A. El-Shaer, M. Al-Suleiman, A. Bakin, A. Waag, A. Voinilovich *et al.*, Appl. Phys. Lett. **91**, 201104 (2007).
[9] S. Heitsch, A. G. Zimmermann, D. Fritsch, C. Sturm, R. Schmidt-Grund, C. Schulz, H. Hochmuth, D. Spemann, G. Benndorf, B. Rheinlnder *et al.*, J. Appl. Phys. **101**, 083521 (2007).
[10] M. Grundmann and C. P. Dietrich, Appl. Phys. Lett. **106**, 123521 (2009).
[11] T. A. Wassner, B. Laumer, S. Maier, A. Laufer, B. K. Meyer, M. Stutzmann, and M. Eickhoff, J. Appl. Phys. **105**, 023505 (2009).
[12] A. Chernikov, S. Horst, M. Koch, K. Volz, S. Chatterjee, S. W. Koch, T. A. Wassner, B. Laumer, and M. Eickhoff, J. Lumin. **130**, 2256 (2010).
[13] W. Shan, W. Walukiewicz, J. W. Ager III, K. M. Yu, H. B. Yuan, H. P. Xin, G. Cantwell, and J. J. Song, Appl. Phys. Lett. **86**, 191911 (2005).
[14] M. Cobet, C. Cobet, M. R. Wagner, N. Esser, C. Thomsen, and A. Hoffmann, Appl. Phys. Lett. **96**, 031904 (2010).
[15] A. Teke, U. Özgür, X. G. S. Doğan, H. Morkoc, B. Nemeth, J. Nause, and H. O. Everitt, Phys. Rev. B **70**, 195207 (2004).
[16] A. Tsukazaki, A. Ohtomo, M. Kawasaki, T. Makino, C. H. Chia, Y. Segawa, and H. Koinuma, Appl. Phys. Lett. **84**, 3858 (2004).
[17] Ü. Oezgür, Y. I. Alivov, C. Liu, A. Teke, M. A. Reshchikov, S. Dogan, and V. Avrutin, S.-J. Cho, and H. Morkoc, Appl. Phys. Lett. **98**, 041301 (2005).
[18] B. K. Meyer, H. Alves, D. M. Hofmann, W. Kriegseis, D. Forster, F. Bertram, J. Christen, A. Hoffmann, M. Straburg, M. Dworzak *et al.*, Phys. Status Solidi B **241**, 231 (2004).
[19] D. G. Thomas, J. Phys. Chem. Solids **25**, 86 (2960).
[20] D. C. Reynolds, D. C. Look, B. Jogai, C. W. Litton, G. Cantwell, and W. C. Harsch, Phys. Rev. B **60**, 2340 (1999).
[21] M. Wagner, G. Callsen, J. Reparaz, J.-H. Schulze, R. Kirste, M. Cobet, I. Ostapenko, S. Rodt, C. Nenstiel, A. Hoffmann *et al.* Phys. Rev. B **847**, 1 (2011).
[22] M. Umlauff, J. Hoffmann, H. Kalt, W. Langbein, J. M. Hvam, M. Scholl, J. Söllner, M. Heuken, B. Jobst, and D. Hommel, Phys. Rev. B **57**, 1390 (1998).
[23] V. V. Travnikov, A. Freiberg, and S. F. Savikhin, J. Lumin. **47**, 107 (1990).
[24] D. C. Reynolds, D. C. Look, B. Jogai, J. E. Hoelscher, and R. E. Sherriff, J. Appl. Phys. **88**, 2152 (2000).
[25] B. Guo, Z. Ye, and K. S. Wong, J. Cryst. Growth **253**, 252 (2003).
[26] K. Kash and J. Shah, J. Lumin. **30**, 333 (1985).
[27] K. Kash, J. Shah, D. Block, A. C. Gossard, and W. Wiegmann, Physica B **134**, 189 (1985).
[28] H. J. Polland, W. W. Rühle, K. Ploog, and C. W. Tu, Phys. Rev. B **36**, 7722 (1987).
[29] M. Kira, F. Jahnke, W. Hoyer, and S. W. Koch, Prog. Quantum Electron. **23**, 189 (1999).
[30] H. Haug and S. W. Koch, *Quantum Theory of the Optical and Electronic Properties of Semiconductors*, 4th ed. (World Scientific, Singapore, 1998).
[31] O. Madelung, *Landolt-Boernstein: Numerical Data and Functional Relationships in Science and Technology* (Springer, Berlin, 1982).
[32] S. Chatterjee, C. Ell, S. Mosor, G. Khitrova, H. M. Gibbs, W. Hoyer, M. Kira, S. W. Koch, J. P. Prineas, and H. Stolz, Phys. Rev. Lett. **92**, 067402 (2004).
[33] R. A. Kaindl, M. A. Carnahan, D. Hägele, R. Lövenich, and D. S. Chemla, Nature **423**, 734 (2003).